Drizzle in stratiform boundary layer clouds. Part II: Microphysical aspects

R. WOOD*

The Met Office, Bracknell, Berkshire, UK.

April 1, 2004

Abstract

This is the second of two observational papers examining drizzle in stratiform boundary layer clouds. Part I details the vertical and horizontal structure of cloud and drizzle parameters, including some bulk microphysical variables. In this paper, the focus is on the *in situ* size resolved microphysical measurements, particularly of drizzle drops ($r > 20\mu$m). Layer averaged size distributions of drizzle drops within cloud are shown to be well represented using a truncated exponential size distribution. The size resolved microphysical measurements are used to validate a number of commonly used bulk microphysical parameterizations of warm rain formation. While parameterized accretion rates agree well with observationally-derived rates, the autoconversion rates seriously disagree in some cases. It is imperative that these disagreements are addressed before serious consideration is given to large-scale numerical model predictions of the aerosol second indirect effect. Cloud droplet coalescence removal rates and mass and number fall rate relationships used in the bulk microphysical schemes are also validated, revealing some potentially important discrepancies. The relative roles of autoconversion and accretion are estimated by examination of composite profiles from the flights. Autoconversion, although necessary for the production of drizzle drops, is much less important than accretion throughout the lower 80% of the cloud layer in terms of the production of drizzle liquid water. The autoconversion rate is found to depend strongly upon the cloud droplet concentration N_d such that a doubling of N_d would lead to a reduction in autoconversion rate of between 2 and 4.

Radar reflectivity-precipitation rate (Z-R) relationships suitable for radar use are derived and are shown to be significantly biased in some cases by the undersampling of large ($r > 200\mu$m) drops with the 2D-C probe. A correction based upon the extrapolation to larger sizes using the exponential size distribution changes the Z-R relationship, leading to the conclusion that consideration should be given to sampling issues when examining higher moments of the drop size distribution in drizzling stratiform boundary layer clouds.

*Current author address: Atmospheric Sciences, Box 351640, University of Washington, Seattle, WA, 98102, USA. BRITISH CROWN COPYRIGHT

1. Introduction

In part I of this study (Wood, 2004b) 12 cases of drizzling stratiform boundary layer clouds were examined, with focus on the horizontal and vertical structure of cloud and drizzle. We extend the study in part II, with a focus upon size resolved microphysical observations, particularly of drizzle drops (drop radius $r > 20\mu$m). Cloud microphysical processes are at the heart of many of the current problems associated with aerosol-cloud-climate interactions (Hobbs, 1993; Beard and Ochs, 1993). There is a growing need to understand the microphysical role of drizzle in marine boundary layer (MBL) clouds. Recent observations (e.g. Bretherton et al., 1995; Miller and Albrecht, 1995; Yuter et al., 2000; Stevens et al., 2003; Bretherton et al., 2004, see also part I of this study) are demonstrating both ubiquity and energetic importance of drizzle in MBL clouds. The amount of drizzle appears to be modulated by cloud microphysics (Hudson and Yum, 2001; Bretherton et al., 2004), and it is therefore imperative that accurate parameterizations of the drizzle process are incorporated into cloud models (Stevens et al., 1998), if such models are to accurately prognose cloud structure and evolution, and to quantify climate feedbacks.

The majority of existing microphysical warm rain parameterizations are based on the general paradigm, first introduced by Kessler (1969), of treating the condensed water in the cloud as belonging to one of two drop populations: cloud drops and rain drops. The former are assumed to be small enough that they do not fall under gravity, whereas the latter have an appreciable terminal velocity. Rate equations are then derived that describe the transfer between the drop populations. Because of its inherent simplicity, this *Kessler paradigm* has been widely adopted

for the parameterization of rain in all the model frameworks described above (e.g Tripoli and Cotton, 1980; Baker, 1993; Beheng, 1994; Rotstayn, 1997; Wilson and Ballard, 1999; Khairoutdinov and Kogan, 2000; Liu and Daum, 2004). Although other methods exist to parameterize rain, they are generally considerably more computationally expensive (e.g. Tzivion et al., 1987) because they explicitly solve the stochastic collection equation. The rate terms for the different parameterizations vary widely in their dependence upon cloud droplet concentration and liquid water. Figure 1 demonstrates just how variable these rate terms are. For typical droplet concentrations and liquid water contents in MBL clouds, the autoconversion rates from different parameterization vary over three orders of magnitude. This stems primarily from the different assumptions made in the generation of the parameterizations. For example, the Beheng and Kessler parameterizations were derived for clouds with generally higher liquid water contents than stratocumulus. What we should conclude from this comparison is that there is a pressing need to attempt to validate the parameterizations in different cloud systems, and ask which of them can be used to simulate the drizzle process most accurately. In this study, we attempt to validate some of the widely used parameterizations of the *Kessler* form using aircraft *in-situ* size-resolved microphysical data. We will also compare accretion rates and fall speed relationships.

Microphysical properties of drizzle are of particular importance for the remote sensing problem, especially with the increasing use of ground-based cloud and rain radars in the study of marine boundary layer cloud (Frisch et al., 1995; Yuter et al., 2000; Comstock et al., 2003). In addition, programs are already underway that will mount sensitive millimeter cloud/drizzle

radars on spaceborne platforms (e.g. the Cloudsat mission, Stephens et al. (2002) and the upcoming European EarthCARE program). There is therefore a need to establish retrieval methods for drizzle so that quantitative large scale observations of drizzle in marine boundary layer clouds can begin. Technical limitations will not permit these pioneering spaceborne platforms to make spectral radar measurements such as those employed in the state of the art ground based radar (Frisch et al., 1995) and so retrieval of precipitation rate will rely upon reflectivity alone. Thus, there is a pressing need to investigate reflectivity-rain rate ($Z - R$) relationships in drizzling boundary layer cloud using in-situ and ground-based remote sensing measurements. We use aircraft data in this study to examine the links between radar reflectivity and precipitation rate.

This study effectively consists of five sections. In section 2 we describe the measurements of the drizzle drop size distribution (DDSD) and examine the most suitable mathematical form for the description of the DDSD. In section 3 we focus upon validation of drizzle parameterizations. Section 4 examines the relative roles of autocoversion and accretion. Section 5 examines $Z - R$ relationships. The study concludes with a brief discussion of the findings.

2. Drizzle drop size distribution

The instruments used to sample the cloud and drizzle size distributions dN/dr were described in Part I of this study. Measurements are made using a PMS Forward Scattering Spectrometer Probe (FSSP, Baumgardner et al. (1993)) and PMS 2D-C optical array probe. The drop radius measurement range spans 1-400 μm. Combined FSSP and 2D-C size distributions are produced

by linear interpolation in log(dN/dr)-log(r) coordinates.

Here, we take a more focused look at some of the sampling issues, and the form that the drizzle drop size distribution (DDSD) takes in stratiform boundary layer clouds. Drizzle drops are defined as those with $r > 20\mu$m. In this section, we examine the mathematical form of the DDSD, and ask how well we are able to determine the moments of the DDSD, particularly the higher moments that are necessary in making estimations of the precipitation rate and radar reflectivity.

The $n-$th complete moment M_n of a drop size distribution dN/dr is defined as

$$M_n = \int_{r=0}^{\infty} r^n \frac{dN}{dr} dr \tag{1}$$

with radar reflectivity $Z = 2^6 M_6$, and liquid water content $q_L = (4\pi/3)\rho_w M_3$, where ρ_w is the (constant) density of liquid water. Partial moments are used to determine cloud ($1 < r < 20\mu$m) and drizzle ($20 < r < 400\mu$m) physical parameters.

We take size distributions from the same horizontal layer averages as discussed in Part I. As we shall see, long averaging times are required to sample the larger drizzle drops that can often contribute strongly to the rain rate, and particularly the radar reflectivity. We analyse DDSD results ($20 < r < 400\mu$m) from all cloud levels, height z, with $0 < z_* < 1$, where $z_* = (z - \overline{z_{CB}})/(\overline{z_i} - \overline{z_{CB}})$, and with z_{CB} and z_i being the cloud base and top heights respectively. For each measured DDSD, we estimate the drizzle drop concentration $N_{d,D}$ and mean radius $\overline{r_D}$. We test how well an exponential DDSD represents these data by first normalizing r and dN/dr. Because our DDSD is necessarily truncated (by design) at $r = r_0 = 20\mu$m, the truncated

exponential form is

$$\left(\frac{dN}{dr}\right)_{exp} = \frac{N_{d,D}}{\overline{r_D} - r_0} \exp\left(\frac{r - r_0}{\overline{r_D} - r_0}\right). \quad (2)$$

where $\overline{r_D}$ is the mean radius of the $r > 20\mu$m drizzle drops. Setting $\mathcal{N} = N_{d,D} \exp(r_0/[\overline{r_D} - r_0])$ and $\mathcal{R} = \overline{r_D} - r_0$, we plot in Fig. 2 normalized DDSD from the entire 12 cloud dataset (103 DDSDs). The collapsed exponential curve $(dN/dr)_{exp} = \mathcal{N}/\mathcal{R} \exp(-r/\mathcal{R})$ provides a good fit to the normalized spectra indicating that the truncted exponental form is a good mathematical descriptor of the DDSD.

Because the exponential provides a good representation of the data, we use the exponential form to assess sampling problems of large drops that stem from the limited sample volume of the 2D-C probe (< 5 litre s^{-1}). Because of this, and the steep fall-off of the exponential distribution, very few drops with radii larger than 200 μm were measured on any of the flights. We therefore extrapolate the exponential out to sizes larger than those measured and calculate the contribution to Z and precipitation rate R from droplets 60 μm$< r < \infty$, and compare with the contribution only over the measured range. To find the best-fit exponential, we use non-linear least squares fitting over the well sampled drop range $20 < r < 60\mu$m, weighting each size bin using the inverse square of the Poissonian counting error. Rain rate R is estimated using a single drop terminal velocity w_T relationship calculated from a fourth order polynomial fit to log(w_T), log(r) calculated at $T = 280$ K and $p = 900$ hPa using the full Reynolds number approach set out in Pruppacher and Klett (1997). Tests show that the terminal velocities calculated using the single fitted curve differ by no more than 5% from those calculated using

the full theory at all the temperatures and pressures experienced in this study.

Figure 3 shows two examples of the procedure. The size distributions are shown in the upper panels for two cases. The second row shows the size-resolved reflectivity spectra dZ/dr (filled circles) and precipitation rate spectra dR/dr (diamonds). The exponential fits are shown with dotted (dZ/dr) and dashed (dR/dr) lines, extrapolated to larger sizes. For the case A644 dZ/dr and dR/dr continues to increase beyond the actual measurements, whereas for A764 the peaks in both dZ/dr and dR/dr are well resolved. The lower panels show the cumulative contribution to dBZ (10log$_{10}Z$+180) and R from 60 μm upwards. In the A644 case the extrapolated dBZ is around 7 dBZ higher (a factor of 5 in Z) than that measured with the 2D-C probe and R is more than doubled. For the A764 case there is only a negligible difference between the extrapolated and measured dBZ and R. Insofar as we can assume the droplets are exponentially distributed, for the A644 case it is likely that droplets larger than those measured may be contributing significantly to the radar reflectivity and precipitation rate whereas in the A764 case this is unlikely. We assess the broader consequences of this undersampling problem in Section 5.

3. Parameterization of cloud microphysical processes

The size-resolved microhysical data are used to validate existing, widely used parameterizations of the *Kessler* type. Five parameterization schemes are explored, each of which have somewhat different dependencies upon cloud microphysical properties. The parameterizations we validate are (a) Khairoutdinov and Kogan (K+K, Khairoutdinov and Kogan, 2000), (b) Kessler (KES, Kessler, 1969), (c) Beheng (BEH, Beheng, 1994), (d) Tripoli and Cotton (T+C, Tripoli and

Cotton, 1980), (e) Liu and Daum (L+D, Liu and Daum, 2004). Table 1 gives the mathematical description of the schemes, and additional assumptions made. For T+C we choose a threshold radius of 7 μm for determination of the liquid water content threshold. This is a fairly common choice when applying this scheme in numerical models (e.g. Jones et al., 2001). The L+D parameterization requires an estimate of the sixth moment of the cloud droplet size distribution, which is expressed by defining $R_6 = \{[\int_0^{r_0} r^6 (dN/dr) dr]/N_d\}^{1/6}$, dN/dr being the number concentration of cloud droplets in the radius range r to $r + dr$, N_d the cloud droplet concentration, and r_0 the largest cloud droplet size (here r_0 is taken to be 20 μm). We parameterize R_6 as a function of the mean volume radius r_v, via $R_6 = \beta_6 r_v$, assuming a modified gamma droplet size distribution (see e.g. Austin et al., 1995) with the spectral width parameterization of Wood (2000). A good fit to the analytical form of this relationship is $\beta_6 = [(r_v + 3)/r_v]^2$, with r_v in microns. An analytical form for the threshold radius R_{6C} is presented in Liu et al. (2004), and is well approximated by $R_{6C} = 7.5/(q_L^{1/6} R_6^{1/2})$, where q_L is in units of kg m^{-3} and R_6 is in μm.

For each measured cloud and drizzle drop size distribution, we estimate autoconversion an accretion rates using an accurate solution of the stochastic collection equation (SCE). We calculate drop coalescence rates with observed droplet size distributions as input to an accurate numerical SCE solver using the mass-conservative flux method of Bott (1998). This scheme has the advantage over previous schemes (e.g. Berry and Reinhardt, 1974) in that it can be operated using a longer timestep (10 seconds) without significant loss of accuracy. The scheme has been successfully verified against both analytical solutions of the SCE, using the Golovin coalescence kernel (Golovin, 1963) and against the Berry-Reinhardt scheme (Bott, 1998). The

model uses the hydrodynamic kernel and collision effi ciencies of Hall (1980), Davis (1972) and Jonas (1972). The drop size distribution is fi rst binned onto logarithmically spaced bins, with the mass increasing by a factor $2^{1/2}$ from one bin to the next). There are 60 size bins, with drop radii from 1.93-1758 μm.

Sedimentation rates for mass and drizzle drop number concentration are also estimated. More complete details are given in the individual subsections below. We then compare the process rates with those from the bulk formulations in the parameterization schemes and investigate discrepancies.

a. Autoconversion

Autoconversion rate is estimated by integration of the SCE as described above, but with only drops $r < 20\mu$m in the initial size distribution, in a manner identical to (Austin et al., 1995), i.e. by calculating the near-linear rate of drizzle ($r > 20\mu$m) mass increase over 10 minutes of (SCE) integration. We expect this to result in more accurate autoconversion rates than the instantaneous method used by (Baker, 1993). Austin et al. (1995) compared their method with the method of (Berry and Reinhardt, 1974), who used the time taken for the mass-weighted mean radius to reach 50 μm, and found differences of around a factor of two (Austin et al. autoconversions being lower). We conclude that the observationally estimated autoconversiom rates are probably accurate to no better than a factor of two.

Figure 4 compares autoconversion rates calculated using the observed data (abscissae) against the parameterised autoconversion rates (ordinates) for the fi ve schemes. There is considerable

variation in the rates for the different parameterisations, which is hardly surprising given the differences in dependencies upon cloud liquid water and droplet concentration between schemes (Table 1). The schemes (KES, T+C and L+D) that have threshold liquid water contents below which no autoconversion takes place tend to considerably overestimate autoconversion rates when the threshold is exceeded. Indeed the threshold in KES is so high that autoconversion is prohibited in many cases. The threshold radius used in T+C has little physical meaning, and tends to be set to low values so that autoconversion is not entirely prohibited in shallow clouds occurring in large scale numerical models.

The L+D autoconversion rates are too large, but by reducing the constant term E (Table 1) to 12% of the published value (Fig. 4(f)), excellent agreement with observations is obtained. The good performance of L+D is a result of using a more physically realistic dependence of the collection kernel upon droplet radius to derive the analytical form for the autoconversion rate than has been used in previous parameterizations (see Liu and Daum, 2004, for a discussion). The reason for near constant overprediction in the published L+D parameterization results from the fact that L+D use a form of the SCE that estimates the total rate of mass coalescence rather than the rate of coalescence mass flux across a threshold radius. This assumption is necessary in order to derive an analytical form for the autoconversion rate, but can be shown to overpredict the rate of autoconversion as defined in this paper by approximately an order of magnitude (Wood, 2004a). Fairly good agreement between observed and parameterised autoconversion rate is found for K+K, the parameterization derived using large eddy simulations with bin resolved microphysics. This suggests that the scope of the K+K parameterization may extend

beyond its intended use only as a bulk parameterization in high resolution numerical models.

Using the observations we attempt to determine the sensitivity of the autoconversion rate to the cloud droplet concentration N_d. We make the supposition that we can represent the autoconversion rate $AUTO$ as a function only of cloud liquid water content q_L and cloud droplet concentration N_d, i.e. $AUTO = Kq_L^a N_d^b$ and attempt to remove the q_L dependence to determine the dependence upon N_d as a residual. Figure 5(a) shows the estimated $AUTO/q_L^a$ ($a = 3$) against q_L normalized with the cloud layer mean value $\overline{q_L}$ in each case. This value of a best removes the q_L dependence, especially for $q_L/\overline{q_L} > 0.5$ (i.e. higher up in the cloud where the autoconversion rate is important). This is demostrated by the relative lack of systematic dependence of $AUTO/q_L^a$ upon q_L for each case. We then plot the logarithmic mean of $AUTO/q_L^a$ against the mean N_d for each of the 12 cases in Fig. 5(b). These values scale well with N_d, and linear regression in log-log space gives $b = -1.5 \pm 0.4$. The best estimate gives $K = 1.6 \times 10^{13}$ kg^{-2} m$^{1.5}$ s^{-1}. We also performed multiple regression in log-log space of q_L, N_d and $AUTO$ which gives $a = 2.8 \pm 0.4$, $b = -1.4 \pm 0.3$ (all errors at the 2-σ level), values somewhat consistent with the residual analysis above. The results confirm that there is a strong, statistically significant dependence of the autoconversion rate upon cloud microphysics.

The observationally-estimated value of a is higher than the exponents in KES ($a = 1.0$), T+C ($a = 2.33$), K+K ($a = 2.47$), and much smaller than that in BEH ($a = 4.7$), and is most consistent with L+D ($a = 3$). The observed value of b is close to the values in L+D ($b = -1$) and K+K ($b = -1.79$), much higher than those in KES ($b = 0$) and T+C ($b = -1/3$), and considerably lower than BEH ($b = -3.3$). We therefore conclude that the modified form of

the L+D parameterization is currently the most accurate Kessler-type autoconversion parameterization with the most realistic dependencies upon cloud liquid water content and droplet concentration. However, further investigation is required to remove the need to arbitrarily tune the constant factor.

We also found that the rate of increase of drizzle droplet concentration $N_{d,D}$ due to autoconversion is well modelled with the assumption that newly formed drizzle droplets have a mean volume radius $r_{new} = 22$ μm, so that the rate can be written as a function of the autoconversion rate

$$\left(\frac{\partial N_{d,D}}{\partial t}\right)_{\text{AUTO}} = \frac{3}{4\pi\rho_w r_{new}^3}\left(\frac{\partial q_{L,D}}{\partial t}\right)_{\text{AUTO}}. \quad (3)$$

Our value of r_{new} differs from that in Khairoutdinov and Kogan (2000) who suggest $r_{new} = 25$ μm, which leads to a 30% smaller rate. However, the value of r_{new} and the drizzle drop concentrations are fairly sensitive to the choice of threshold radius (here 20 μm) and the choice of discrete size bins used in the autoconversion calculations. We find that the value of r_{new} is only slightly larger (by a few percent) than the centre of the smallest radius bin classified as drizzle.

b. Accretion

Accretion rates were derived in the same manner as autoconversion rates by integration of the SCE except that the full droplet size distribution was used. The rate of drizzle droplet mass increase thus obtained is that due to the combined effects of autoconversion and accretion, and

so we calculate the latter by subtraction of the derived autoconversion rate from the combined rate.

Accretion rates are compared in Fig. 6. The parameterisation schemes tend to perform better than for autoconversion rate, with T+C being the least biased. Biases in the other schemes do not exceed 70%, which is encouraging. For reasons mentioned above the autoconversion rates (and also accretion rates) are likely to be accurate to no better than a factor of two. The formulations for accretion rate all have similar dependencies upon cloud and drizzle liquid water content.

The rate of loss of cloud droplets is parameterized in K+K by assuming that all collected drops (through both autoconversion and accretion) have a size equal to the mean volume radius of the cloud droplets. Such rates are important for the investigation of aerosol scavenging effects and the associated transition from a polluted to a clean boundary layer. We test this by comparison with the rate of cloud droplet loss using the SCE integrations. We should note that K+K does not take into account self-collection, i.e. the loss of drops by coalescing cloud drops that do not produce a drizzle drop. Results suggest however, that although cloud droplet loss by self-collection is often comparable to or larger than that by autoconversion, it is accretion that tends to dominate the removal of cloud drops. Thus, the self-collection contribution to the overall cloud droplet loss rate is small. We use the observationally-derived autoconversion and accretion rates to avoid the aliasing of biases we have already discussed in these rates, and concentrate only on the parameterized cloud droplet loss rates. Figure 7(a) shows the rates derived from the observed drop size distributions against the parameterization. For observed droplet loss rates higher than around 100 m^{-3} s^{-1} the rates in most cases agree to within a

factor of two. For lower loss rates the parameterization tends to overestimate the rate of droplet loss. However, a droplet loss rate of 100 m^{-3} s^{-1} means that in one hour only 0.36 cloud droplets are lost to autoconversion/accretion which is rather insignifi cant.

We also compare our cloud droplet loss rates with those from BEH which has separate rates for the loss due to autoconversion, accretion and self-collection. The droplet loss rates for autoconversion and accretion rates are presented in BEH as a function of the mass autoconversion and accretion rates, and as with the K+K comparison, we use the observationally-derived values. We compare the total rate of cloud droplet loss in Fig. 7(b) for BEH. As with K+K, these compare favorably at larger rates, and there is a tendency for overprediction especially at the smaller rates. Neither T+C or KES include terms to account for removal of cloud droplets due to the coalescence mechanism.

c. Sedimentation

Parameterization of the drizzle process requires expressions for the rate at which the droplet population sediments. Given that the drizzle droplet population is well modelled using an exponential distribution, parameterization of drizzle drop sedimentation rates will require specifi cation of the rate at which both the drop number and a second moment of the distribution falls (i.e. a two-moment parameterization of the DDSD). The mass fall rate is simply the precipitation rate R defi ned as

$$R = R_{mass} = \frac{4\pi\rho_w}{3}\int_0^\infty w_T r^3 \frac{dN}{dr} dr, \tag{4}$$

and the number fall rate is

$$R_{number} = \int_0^\infty w_T \frac{dN}{dr} dr. \tag{5}$$

We have plotted the mass and number fall speeds as parameterized using K+K against the observed ones in Fig. 8. In most cases these agree to within a factor of two. Note that in all cases, the observed fall rates include the contribution from the exponential extrapolaion at large sizes. The K+K precipitation rates are generally slightly lower and the number rates slightly higher than those from the observations. The cause of these differences is not clear but may include differences in the drop terminal velocity relationships used in both cases.

4. Relative roles of autoconversion and accretion

The relative importances of autoconversion and accretion in determining the increase in drizzle liquid water content is an interesting issue that has received little specific attention in the literature. Results presented in section 3a suggest that autoconversion rates depend strongly upon the liquid water content, and therefore height in the cloud. Accretion rates depend not only upon cloud ($r < 20\mu$m) microphysical parameters (N_d, q_L), but also upon the drizzle liquid water content which has a broad peak in the centre of the cloud (see part I of this study). Figure 9 shows a composite of normalized profiles of autoconversion and accretion. To construct the plot we use the autoconversion and accretion rates derived from the observations (Section 3a,b). For each flight we normalize the autoconversion rates by the cloud mean values and then bin the data from all the flights into normalized height bands. The normalized

height $z_* = (z - \overline{z_{CB}})/(\overline{z_i} - \overline{z_{CB}})$, where $\overline{z_{CB}}$ and $\overline{z_i}$ are the mean cloud base and cloud top respectively.

Autoconversion rate increases rapidly with height in the cloud. A linear increase of cloud liquid water content with height, a constant droplet concentration, and autoconversion rates that depend upon q_L to some power β, leads to curves of the form shown by the dashed lines, for values of $\alpha = 1, 2, 3, 4$. The observed increase in autoconversion rate with z_* is consistent with $2 < \alpha < 3$ discussed in Section 3a above. Accretion rates peak further down in the cloud at around $z_* = 2/3$. The lower panels in Fig. 9 show the relative contribution to the total rate of increase of drizzle liquid water content (autoconversion+accretion) from the two processes. Accretion dominates the production of $q_{L,D}$ throughout most of the cloud. Autoconversion only becomes a significant process in the upper 20% of the cloud. Even in these upper levels accretion still plays a significant role. Because autoconversion rates are significant only in a thin layer of cloud, its parameterization in numerical models with coarse vertical resolution is likely to be particularly problematic and may suggest why some of the commonly used parameterizations require considerable tuning when used in such models (Pincus and Klein, 2000; Rotstayn, 2000).

5. Radar reflectivity-precipitation rate relationships

With the increasing use of radars to measure stratocumulus cloud and precipitation properties from both the ground (e.g. Frisch et al., 1995; Yuter et al., 2000) and from space (e.g. the upcoming Cloudsat mission), there is a need to understand the relationships between parameters

measured with the radar and physically significant cloud properties. Precipitation rate is one of the key properties that has great implications for the hydrological cycle and for the dynamics of the boundary layer. It is therefore not surprising that relationships between radar reflectivity and precipitation rate ($Z - R$ relationships) have been most scrutinised, albeit in most cases for clouds with significantly higher precipitation rates than are found in stratocumulus cloud (e.g. Stout and Mueller, 1968). The measurements presented in this study offer the opportunity of investigating such relationships in stratocumulus cloud.

We present measurements from all in-cloud levels in all flights in Fig. 10, in the form of a comparison of the total dBZ calculated from the extrapolated exponential (60 μm$< r < \infty$, ordinate) and from the uncorrected 2D-C data (abscissa). The dashed line shows exact agreement and the dotted lines represent the extrapolated exceeding the data by 2.5, 5 and 7.5 dBZ. It is clear that for the majority of flights the differences are small (less than 2.5 in many cases). However, there is a tendency for poorer agreement at larger values of dBZ, i.e. for the heavier drizzle cases. We do not include levels below cloud because evaporation of the smaller droplets tends to result in non-exponential size distributions. We did not include flight A641 in this comparison because this flight contained low amounts of drizzle droplets and dN/dr at large drop size was noisy and was not well modelled with an exponential. We do not show the comparison between precipitation rates but the behaviour is qualitatively similar to that for dBZ. The fractional increase in Z from the data to the exponential extrapolation is a factor of 1.0 to 3.0 times the fractional increase in R. Because the value of this factor is positively correlated with high values of R there are important consequences for the true $Z - R$

relationships in drizzling stratocumulus.

Values of R and Z are derived for the droplet size distribution over the size range $r > 20$ μm in two ways. The first method is a direct calculation from the measured size distribution giving values R_{data} and Z_{data}. The second uses the exponentially fitted size distribution for $r > 60$ μm drops and the measured values for $r \leq 60$ μm, giving values R_{exp} and Z_{exp}. For flight A641 we use only the measured size distribution for reasons mentioned above and so the two methods yield the same values of Z and R. We use least squares fitting to obtain the parameters a and b in the relationship $Z = aR^b$. Table 2 shows the values of a and b for the fits, along with the estimated errors (2-σ level) and the regression coefficient r^2. The most important difference between the relationships is that the exponent b is larger for the extrapolated data ($b = 1.18$) than the measured data ($b = 1.04$). This is a direct result of there being larger fractional increases in Z than in R for the extrapolated distributions compared with the measured ones. These values of a and b for the extrapolated distributions $Z - R$ relationship compare well with those derived derived from millimeter cloud radar data taken in drizzling stratocumulus over the SE Pacific Ocean (Comstock et al., 2003), suggesting that there may be a universal nature to drizzle from stratiform marine boundary layer cloud.

Figure 11 shows the $Z_{exp} - R_{exp}$ relationship for all in-cloud cases. The value of r^2 for the log-log fit is 0.89. These results suggest that, although there is a good correlation between radar reflectivity and precipitation rate, the relationship is not a unique one. Additional information about the drop size distribution will improve the relationship. Retrievals of precipitation rate from radar reflectivity alone will incur considerable error (Fig. 11), possibly as much as a factor

of 2 or 3 in precipitation rate. With additional information, this error can be approximately halved.

6. Discussion and conclusions

We have investigated some aspects of the size-resolved drizzle microphysics using 12 flights in stratocumulus. The drizzle drop size distribution (DDSD) is found to be well represented using a truncated exponential, and this has been used to correct for the poor sampling of drops larger than $r \sim 200\mu$m. Values of the higher moments of the DDSD necessary to derive radar reflectivity and rain rate are, in some cases, found to be biased by the poor sampling, particularly at higher rain rates.

Values of autoconversion, accretion, and sedimentation rates are derived from the cloud and drizzle drop size distributions and compared to those from five widely used parameterizations. Autoconversion rates compare most favourably with a modified version of Liu and Daum (2004), whereas accretion rate formulations all show good agreement with data, there being less variation in the parameterizations. The data are consistent with a power 2-3 dependency upon cloud liquid water content. We found also a strong and statistically significant dependence of the autoconversion rate upon cloud droplet concentration N_d, with autoconversion rate decreasing markedly with increasing N_d. A doubling of N_d leads to a decrease in autoconversion rate of between 2 and 4, with the range in this estimate related to uncertainties in the relationship between autoconversion and N_d. This suggests a strong role for cloud microphysical properties in the production of drizzle. and confirms the hypothesis that drizzle is suppressed in clouds

with high cloud droplet concentration. Modeling is required to investigate the dynamical and thermoynamical feedbacks associated with suppression. It is found that the accretion rate dominates the production of drizzle liquid water throughout most of the cloud, with autoconversion being dominant at cloud top only. The production of new drizzle drops is dominant at cloud top.

Radar reflectivity-rain rate ($Z - R$) relationships are found to be affected by the sampling problems discussed above. With data corrected for the sampling problems, we find an exponent $b \sim 1.2$ that is smaller than those commonly found in heavier rain $b \sim 1.5$. This relationship is explored further in (Comstock et al., 2003) and is suggestive of a stronger control on rain rate by variations in number concentration of drizzle drops, and less control by the size of drizzle drops, compared to heavier rain. These relationships should prove useful when designing drizzle retrieval methods from surface and satellite radars.

Acknowledgement The author wishes to thank the staff of the Meteorological Research Flight and the C-130 aircrew and groundcrew for their dedication to collecting the data presented in this study. I am grateful to colleagues in the Met Office and elsewhere, for discussions which aided the research presented in this paper. I thank Andreas Bott for provision of the numerical code to solve the SCE.

References

Austin, P., Y. Wang, R. Pincus, and V. Kujala: 1995, Precipitation in stratocumulus clouds: observations and modelling results. *J. Atmos. Sci.*, **52**, 2329–2352.

Baker, M. B.: 1993, Variability in concentrations of cloud condensation nuclei in the marine cloud-topped boundary layer. *Tellus*, **45B**, 458–472.

Baumgardner, D., B. Baker, and K. Weaver: 1993, A technique for measurement of cloud structure on centimeter scales. *J. Atmos. Oceanic Technol.*, **10**, 557–565.

Beard, K. V. and H. T. Ochs: 1993, Warm-rain initiation: An overview of microphysical mechanisms. *J. Appl. Meteor.*, **32**, 608–625.

Beheng, K. D.: 1994, A parameterization of warm cloud microphysical conversion processes. *Atmos. Res.*, **33**, 193–206.

Berry, E. X. and R. L. Reinhardt: 1974, An analysis of cloud drop growth by collection: Part ii. single initial distributions. *J. Atmos. Sci.*, **31**, 1825–1831.

Bott, A.: 1998, A flux method for the numerical solution of the stochastic collection equation. *J. Atmos. Sci.*, **55**, 2284–2293.

Bretherton, C. S., P. Austin, and S. T. Siems: 1995, Cloudiness and marine boundary layer dynamics in the astex lagrangian experiments. Part ii: Cloudiness, drizzle, surface fluxes and entrainment. *J. Atmos. Sci.*, **52**, 2724–2735.

Bretherton, C. S., T. Uttal, . Fairall, C. W., . Yuter, S. E., . Weller, R. A., . Baumgardner, D., . Comstock, K., and R. Wood: 2004, The EPIC 2001 stratocumulus study. *Bull. Am. Meteorol. Soc.*, in press.

Comstock, K., S. Yuter, and R. Wood: 2003, Radar observations of precipitation in and below stratocumulus clouds. *Quart. J. Roy. Meteorol. Soc.*, in review.

Davis, M. H.: 1972, Collisions of small droplets: Gas kinetic effects. *J. Atmos. Sci.*, **29**, 911–915.

Frisch, A. S., C. W. Fairall, and J. B. Snider: 1995, Measurement of cloud and drizzle parameters during astex with a k_α band doppler radar and a microwave radiometer. *J. Atmos. Sci.*, **52**, 2788–2799.

Golovin, A. M.: 1963, The solution of the coagulation equation from cloud droplets in a rising air current. *Izv. Akad. Nauk. SSSR. Ser. Geofiz.*, **5**, 783–791.

Hall, W. D.: 1980, A detailed microphysical model within a two-dimensional dynamic framework: Model description and preliminary results. *J. Atmos. Sci.*, **37**, 2486–2507.

Hobbs, E., P. V.: 1993, *Aerosol-Cloud-Climate Interactions*. Academic Press.

Hudson, J. G. and S. S. Yum: 2001, Maritime-continental drizzle contrasts in small cumuli. *J. Atmos. Sci.*, **58**, 915–926.

Jonas, P. R.: 1972, The collision effi ciency of small drops. *Quart. J. Roy. Meteorol. Soc.*, **98**, 681–683.

Jones, A., D. L. Roberts, M. J. Woodage, and C. E. Johnson: 2001, Indirect aerosol forcing in a climate model with an interactive sulphur cycle. Hadley Centre Technical Note HCTN-25, Meteorological Offi ce.

Kessler, E.: 1969, On the distribution and continuity of water substance in atmospheric circulations. *Meteor. Monogr.*, **32**, Amer. Meteor. Soc. 1–84.

Khairoutdinov, M. and Y. Kogan: 2000, A new cloud physics parameterization in a large-eddy simulation model of marine stratocumulus. *J. Atmos. Sci.*, **57**, 229–243.

Liu, Y. and P. H. Daum: 2004, On the parameterization of the autoconversion process. Part i: Analytical formulation of the kessler-type parameterizations. *J. Atmos. Sci.*, in press.

Liu, Y., P. H. Daum, and R. McGraw: 2004, An analytical expression for predicting the critical radius in the autoconversion parameterization. *Geophys. Res. Lett.*, in press.

Miller, M. A. and B. A. Albrecht: 1995, Surface-based observations of mesoscale cumulus-stratocumulus interaction during astex. *J. Atmos. Sci.*, **52**, 2809–2826.

Pincus, R. and S. A. Klein: 2000, Unresolved spatial variability and microphysical process rates in large scale models. *J. Geophys. Res.*, **105**, 27059–27066.

Pruppacher, H. R. and J. D. Klett: 1997, *Microphysics of clouds and precipitation*. Kuwer Academic Publishers, 976 pp.

Rotstayn, L. D.: 1997, A physically based scheme for the treatment of stratiform clouds and

precipitation in large-scale models. i: Description and evaluation of the microphysical processes. *Quart. J. Roy. Meteorol. Soc.*, **123**, 1227–1282.

— 2000, On the ”tuning” of autoconversion parameterizations in climate models. *J. Geophys. Res.*, **105**, 15,495–15,507.

Stephens, G. L., D. G. Vane, R. Boain, G. Mace, K. Sassen, Z. Wang, A. Illingworth, E. O'Connor, W. Rossow, S. L. Durden, S. Miller, R. Austin, A. Benedetti, C. Mitrescu, and the CloudSat Science Team: 2002, The CloudSat mission and the EOS constellation: A new dimension of space-based observations of clouds and precipitation. *Bull. Amer. Meteorol. Soc.*, **83**, 1771–1790.

Stevens, B., W. R. Cotton, G. Feingold, and C.-H. Moeng: 1998, Large-eddy simulations of strongly precipitating, shallow, stratocumulus-topped boundary layers. *J. Atmos. Sci.*, **55**, 3616–3638.

Stevens, B., D. Lenschow, G. Vali, H. Gerber, B. Bandy, A. Blomquist, J.-L. Brenguier, C. Bretherton, F. Burnet, T. Campos, S. Chai, I. Faloona, D. Friesen, S. Haimov, K. Laursen, D. Lilly, S. Loehrer, S. Malinowski, B. Morley, M. Petters, D. Rogers, L. Russell, V. Savic-Jovac, J. Snider, D. Straub, M. Szumowski, H. Takagi, D. Thornton, M. Tschudi, C. Twohy, M. Wetzel, and M. van Zanten: 2003, Dynamics and Chemistry of Marine Stratocumulus - DYCOMS II. *Bull. Amer. Meteor. Soc.*, **84**, 579–593.

Stout, G. E. and E. A. Mueller: 1968, Survey of relationships between rainfall rate and radar reflectivity in the measurement of precipitation. *J. Appl. Met.*, **7**, 465–474.

Tripoli, G. J. and W. R. Cotton: 1980, A numerical investigation of several factors contributing to the observed variable density of deep convection over south fbrida. *J. App. Meteorol.*, **19**, 1037–1063.

Tzivion, S., G. Feingold, and Z. Levin: 1987, An effi cient numerical solution to the stochastic collection equation. *J. Atmos. Sci.*, **44**, 3139–3149.

Wilson, D. R. and S. P. Ballard: 1999, A microphysically based precipation scheme for the uk meteorological offi ce unifi ed model. *Quart. J. Roy. Meteorol. Soc.*, **125**, 1607–1636.

Wood, R.: 2000, Parametrization of the effect of drizzle upon the droplet effective radius in stratocumulus clouds. *Quart. J. Roy. Meteorol. Soc.*, **126**, 3309–3324.

— 2004a, Comment on "On the parameterization of the autoconversion process. Part I: Analytical formulation of the kessler-type parameterizations". *J. Atmos. Sci.*, submitted.

— 2004b, Drizzle in stratocumulus: Part I: Vertical and horizontal structure. *J. Atmos. Sci.*, submitted.

Yuter, S. E., Y. L. Serra, and R. A. Houze Jr.: 2000, The 1997 pan american climate studies tropical eastern pacifi c process study: Part II. stratocumulus region. *Bull. Amer. Meteor. Soc.*, **81**, 483–490.

Table 1: Autoconversion and accretion formulations for the four parameterisations validated. Units are kg m^{-3} for liquid water contents, m^{-3} for droplet concentrations, and all droplet radius parameters in μm. The air density ρ is expressed in units of kg m^{-3}. $H(x)$ is the Heaviside step function.

Scheme	Autoconversion rate [kg m^{-3} s^{-1}]	Accretion rate [kg m^{-3} s^{-1}]
Khairoutdinov and Kogan (2000)	$Aq_L^{2.47}N_d^{-1.79}\rho^{-1.47}$ ($A = 7.42 \times 10^{13}$)	$67(q_L q_D)^{1.15}\rho^{-1.3}$
Kessler (1969)	B max($q_L - q_{L,0}$,0) ($B = 1.0d - 3$; $q_{L,0} = 5 \times 10^{-4}$)	$0.29 q_L q_D^{7/8} N_d^{1/8}$
Beheng (1994)	$Cd^{-1.7}q_L^{4.7}N_d^{-3.3}$ ($C = 4.8 \times 10^{14}$; $d = 9.9$ for $N_d < 200$ cm^{-3} $d = 3.9$ for $N_d > 200$ cm^{-3})	$6.0 q_L q_D$
Tripoli and Cotton (1980)	$Dq_L^{7/3}N_d^{-1/3}H(q_L - q_{L,0})$ ($D = 3268$, assumes E_C=0.55 $q_{L,0}$ assumes $r_{cm} = 7\mu$m)	$4.7 q_L q_D$
Liu and Daum (2004)	$Eq_L^3 N_d^{-1} H(R_6 - R_{6C})$ ($E = 1.08 \times 10^{10}\beta_6^6$ where $R_6 = \beta_6 r_v$, $\beta_6^6 = [(r_v + 3)/r_v]^2$ (see text), r_v is mean volume radius) $R_{6C} = 7.5/(q_L^{1/6}R_6^{1/2})$	N/A
Liu and Daum (2004) (modified)	as above but $E = 1.3 \times 10^9 \beta_6^6$	N/A

Table 2: Details of the $Z - R$ relationships derived from the measured and extrapolated size distributions. Units are mm^6 m^{-3} (reflectivity) and mm hr $^{-1}$ (preciptitation rate) to retain consistency with other studies. Numbers in parentheses indicate 2-σ errors in a and b (percentage for a, absolute for b).

Relationship	a	b	r^2
$Z_{data} = aP_{data}^b$	6.0	1.04	0.89
	[36.8%]	[0.07]	
$Z_{exp} = aP_{exp}^b$	12.4	1.18	0.88
	[51.6%]	[0.10]	

Figure captions

Figure 1: Comparison of parameterized autoconversion rates from widely used schemes. The upper panel shows autoconversion rate as a function of liquid water content for a fixed cloud droplet concentration of N_d =100 cm^{-3}. The lower panel shows autoconversion rates as a function of droplet concentration for a fixed liquid water content of q_L=0.5 g m^{-3}.

Figure 2: Normalised droplet spectra $(\mathcal{R}/\mathcal{N})dN/dr$ at all in-cloud levels (103 spectra) plotted against $r/\mathcal{R}$. The universal exponential distribution $(\mathcal{R}/\mathcal{N})dN/dr = \exp(-r/\mathcal{R})$ is shown by the dashed line. The spectra are shown by the contours which denote percentiles of all the distributions in each $r/\mathcal{R}$ class. The lightest colored contour therefore contains 95% of all the size distributions in each class.

Figure 3: Examples from two flights showing drop size distributions (a,b), size resolved radar reflectivity dZ/dr and precipitation rate distributions dR/dr (c,d) and the cumulative values of dBZ integrated from $r = 60\mu$m upwards. Data values obtained using the 2D-C and FSSP probes are shown using symbols, and dashed and dotted lines show the fitted exponential distributions. For the $z = 950$ m run in flight A644 (left) the exponential distribution suggests that both Z and R have contributions from drops larger than those actually measured. For the $z = 275$ m run in A764 the measurements capture almost entirely the contributions to Z and R.

Figure 4: Comparison of autoconversion rates derived from the observed droplet size distributions (abscissae) and from the parameterizations of (a) Khairoutdinov and Kogan (2000); (b) Kessler (1969); (c) Beheng (1994); (d) Tripoli and Cotton (1980); (e) Liu and Daum (2004); (f) modified Liu and Daum (2004). Formulations for the parameterized autoconversion rates are presented in Table 1. Points for which the parameterized autoconversion rates are zero are shown along the abscissae. The symbolia are shown in Fig. 6.

Figure 5: (a) Observationally-derived autoconversion rates normalized with q_L^a ($a = 3$) to best remove systematic dependence upon liquid water content. Line and symbol types shown above the plot; (b) normalized autoconversion rates plotted against mean cloud droplent concentration. Symbols are those shown in Fig. refcompacc. Light dashed lines show the power laws with b=-1, -4/3, and -5/3. Heavy dashed line shows best fit from the residual analysis (see text).

Figure 6: As for Fig. 4 but comparing accretion parameterizations.

Figure 7: Comparison of combined autoconversion/accretion rate of loss of cloud droplets derived from the observed droplet size distributions (abscissa) with those parameterized (ordinate) assuming that all collected drops have the size of the mean volume radius of the cloud drops r_v.

Figure 8: Mass (a) and number (b) fall rates as defined in Eqns. 4 and 5 compared with those using the parameterization of Khairoutdinov and Kogan (2000). Dashed lines show perfect agreement; dotted lines show factor of two errors.

Figure 9: Composite profiles from all flights of (a) autoconversion and (b) accretion rate normalized with the flight mean in each case. The lower panels show the fraction of total drizzle liquid water content production rate (autoconversion+accretion) contributed by (c) autoconversion and (d) accretion. In all plots solid circles are median values for each height bin; dashed lines show 25th and 75th percentiles. The dashed curves in (a) show the autoconversion rate expected for a cloud with a linear increase in cloud liquid water content with height and where autoconversion depends upon liquid water content to the power b, with $b = 1, 2, 3, 4$.

Figure 10: Reflectivity factor dBZ derived using droplets with radii larger than 60 μm for data values (abscissa) and for the fitted exponential distributions extrapolated to $r = \infty$ (ordinate). In most cases there is only a small difference between the two values indicating that the 2D-C sample volume is sufficiently large enough to account for significant contributions to reflectivity from all droplet sizes. However, in A644 there are differences of at least 10 dBZ in some cases which arise because drops larger than those measured using the 2D-C are contributing significantly to the reflectivity.

Figure 11: (a) Derived reflectivities Z_{exp} plotted against precipitation rates R_{exp} for all the

in-cloud extrapolated distributions. The dotted line represents the best fit power law with parameters given in Table 2. Symbols are as for Fig. 10.

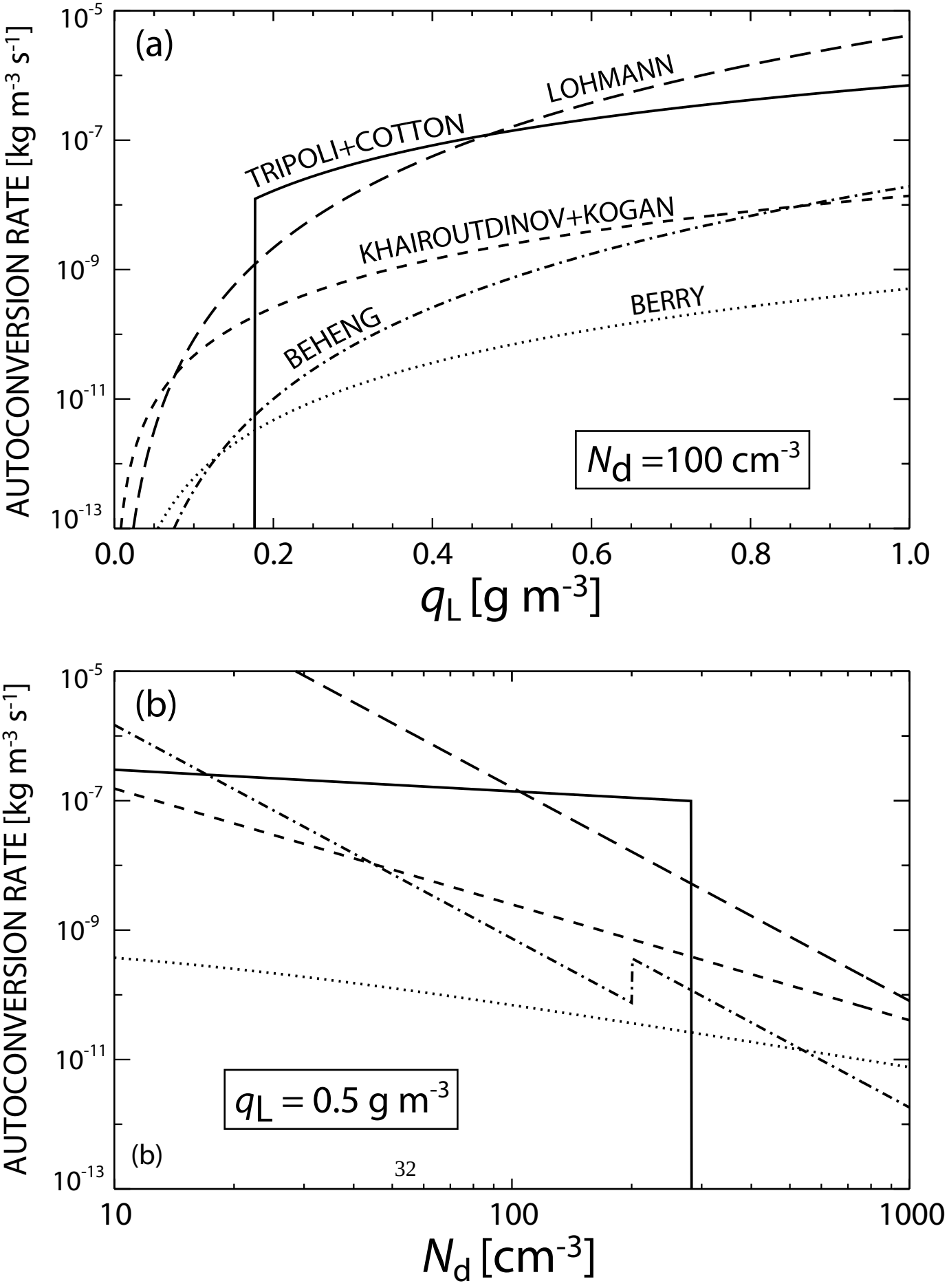
(a)
TRIPOLI+COTTON
LOHMANN
KHAIROUTDINOV+KOGAN
BEHENG
BERRY
N_d =100 cm^{-3}
AUTOCONVERSION RATE [kg m^{-3} s^{-1}]
q_L [g m^{-3}]
(b)
q_L = 0.5 g m^{-3}
N_d [cm^{-3}]

Figure 1:

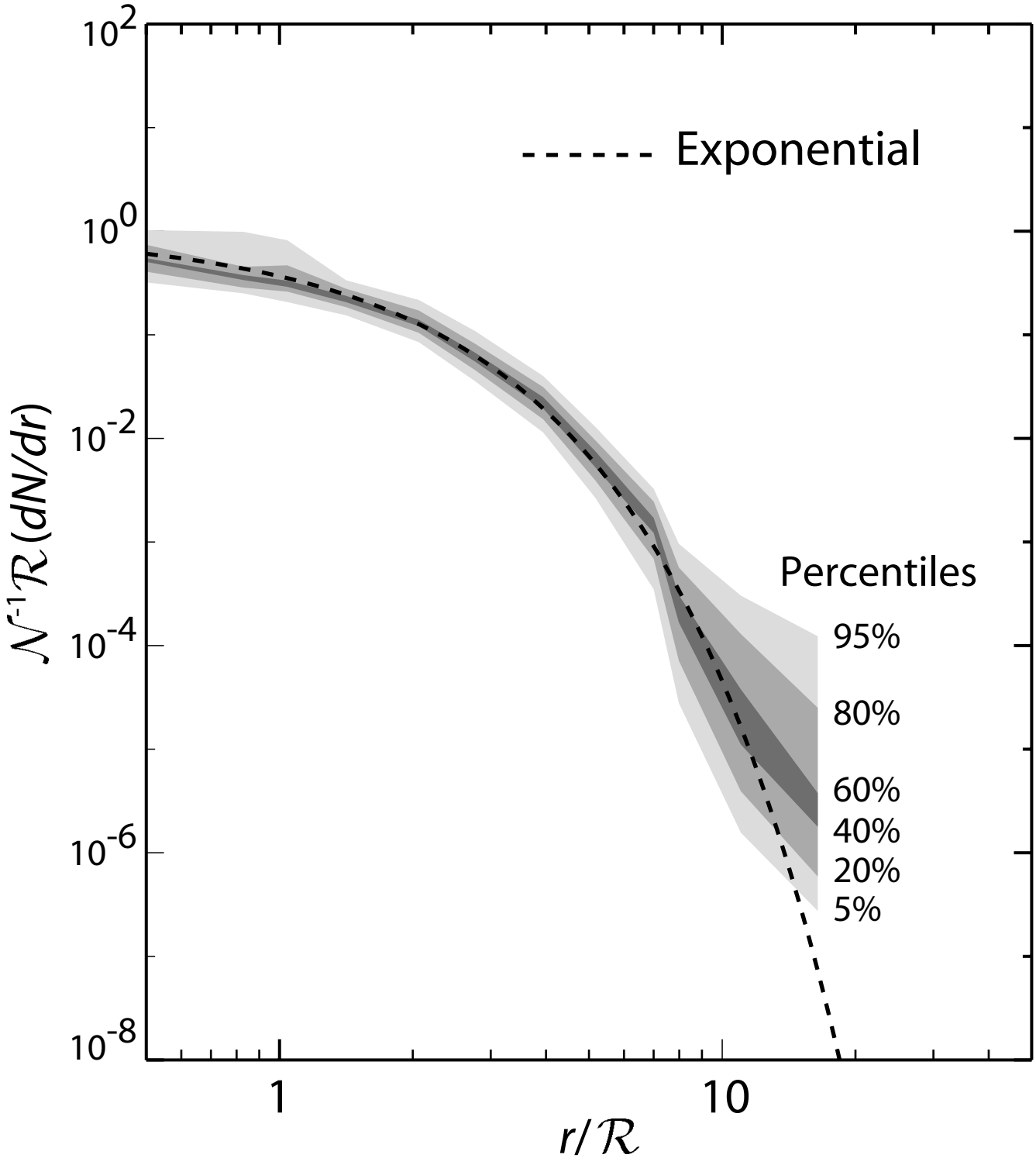
Exponential
Percentiles
95%
80%
60%
40%
20%
5%
10^{2}
10^{0}
10^{-2}
10^{-4}
10^{-6}
10^{-8}
1
10
$r/\mathcal{R}$
$\mathcal{N}^{-1}\mathcal{R}\,(dN/dr)$

Figure 2:

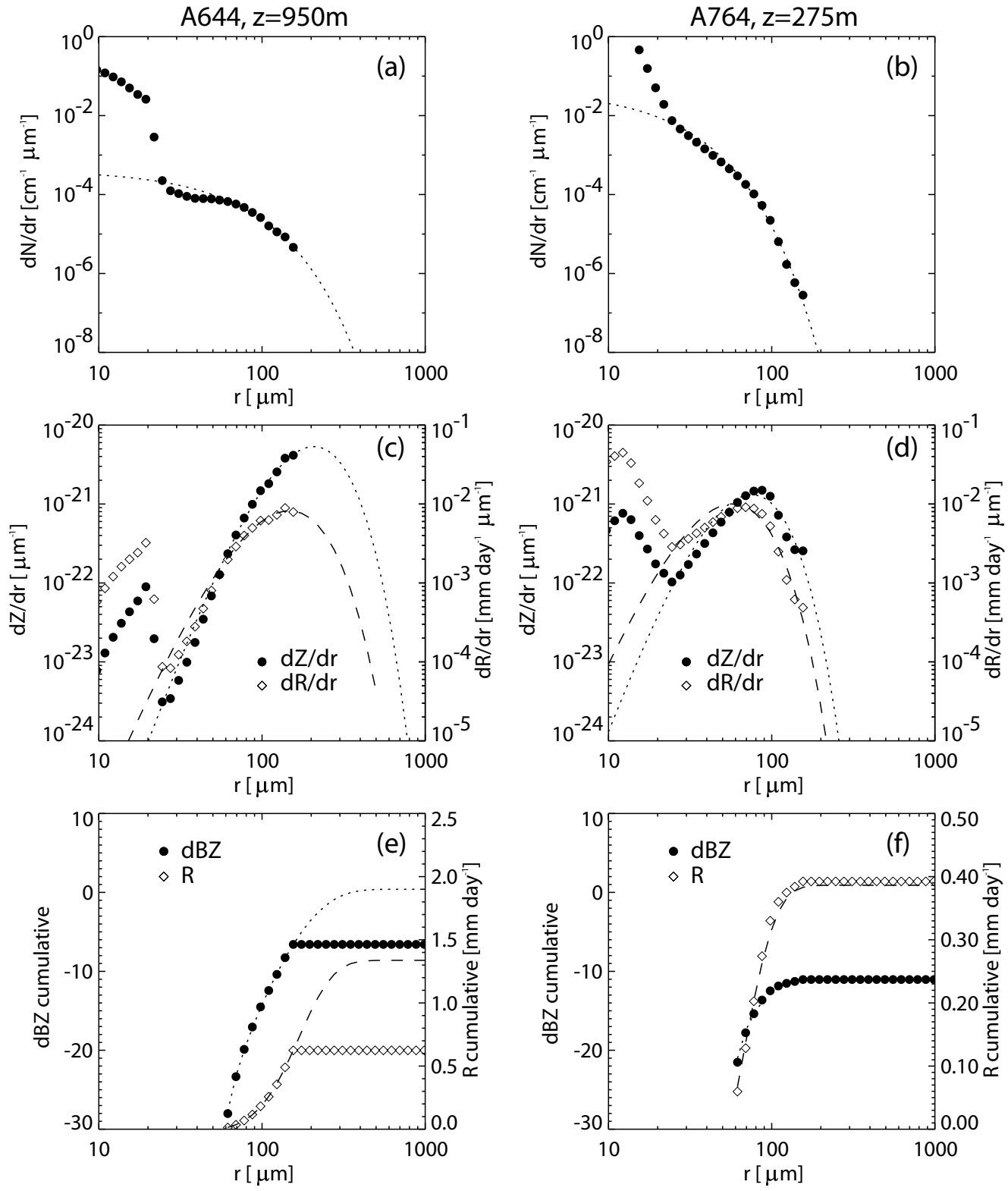
A644, z=950m
A764, z=275m
(a)
(b)
(c)
(d)
(e)
(f)
dN/dr [cm⁻¹ μm⁻¹]
r [μm]
dZ/dr [μm⁻¹]
dR/dr [mm day⁻¹ μm⁻¹]
dZ/dr
dR/dr
dBZ
R
dBZ cumulative
R cumulative [mm day⁻¹]

Figure 3:

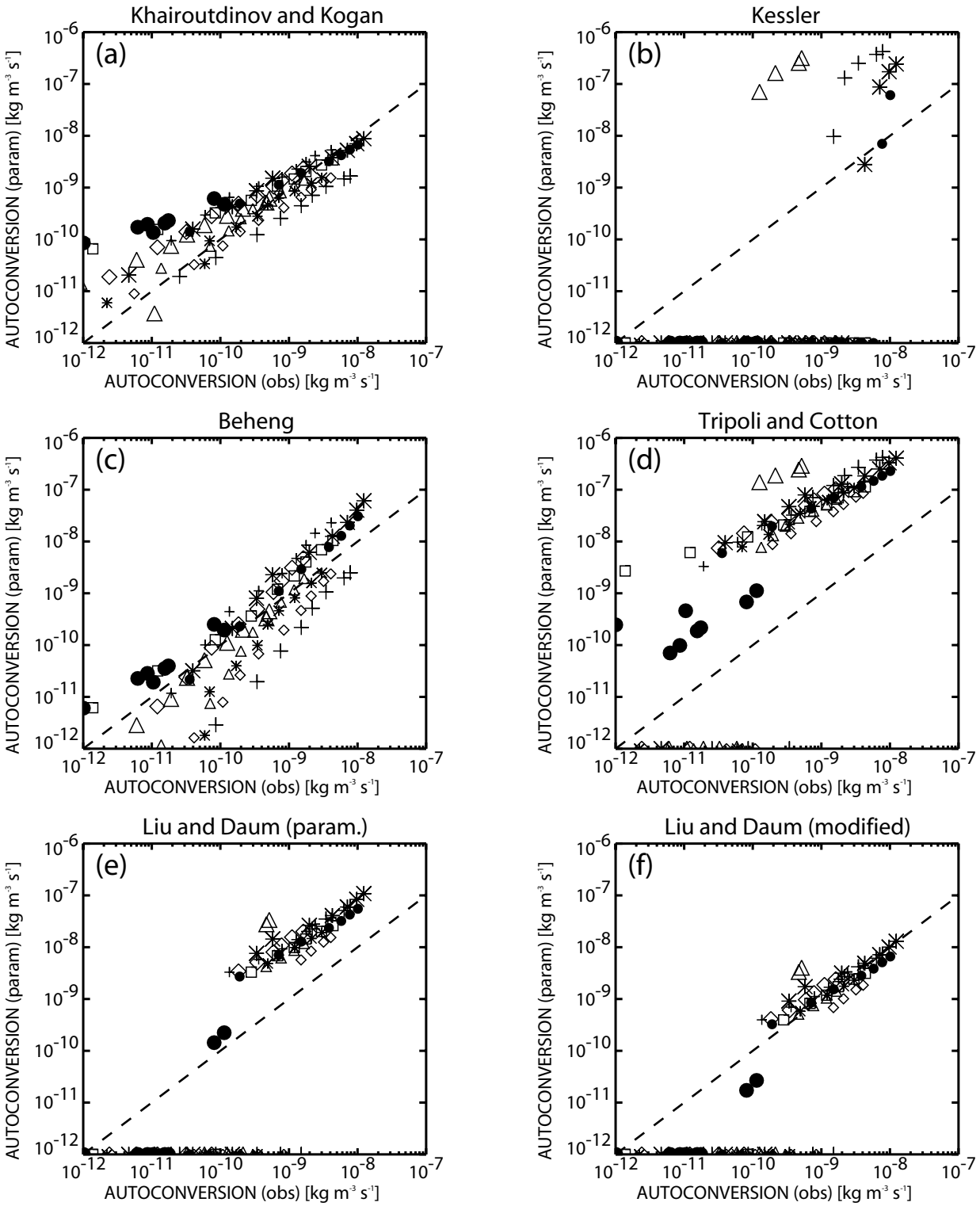
Khairoutdinov and Kogan
(a)
Kessler
(b)
Beheng
(c)
Tripoli and Cotton
(d)
Liu and Daum (param.)
(e)
Liu and Daum (modified)
(f)
AUTOCONVERSION (param) [kg m-3 s-1]
AUTOCONVERSION (obs) [kg m-3 s-1]
10-6
10-7
10-8
10-9
10-10
10-11
10-12

Figure 4:

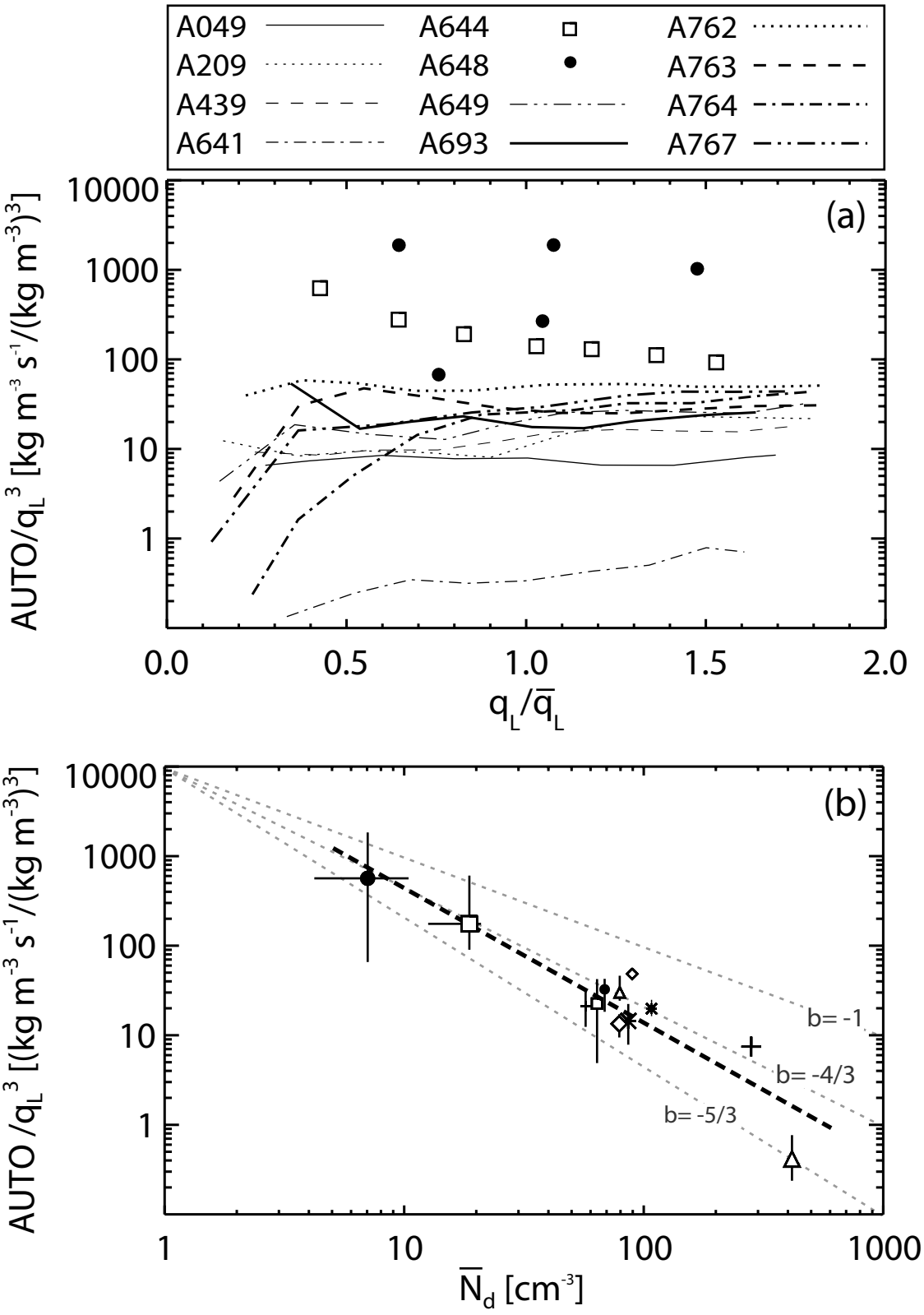
A049
A209
A439
A641
A644
A648
A649
A693
A762
A763
A764
A767
(a)
AUTO/q_L^3 [kg m^-3 s^-1/(kg m^-3)^3]
q_L/q̄_L
(b)
AUTO /q_L^3 [(kg m^-3 s^-1/(kg m^-3)^3]
N̄_d [cm^-3]
b= -1
b= -4/3
b= -5/3

Figure 5:

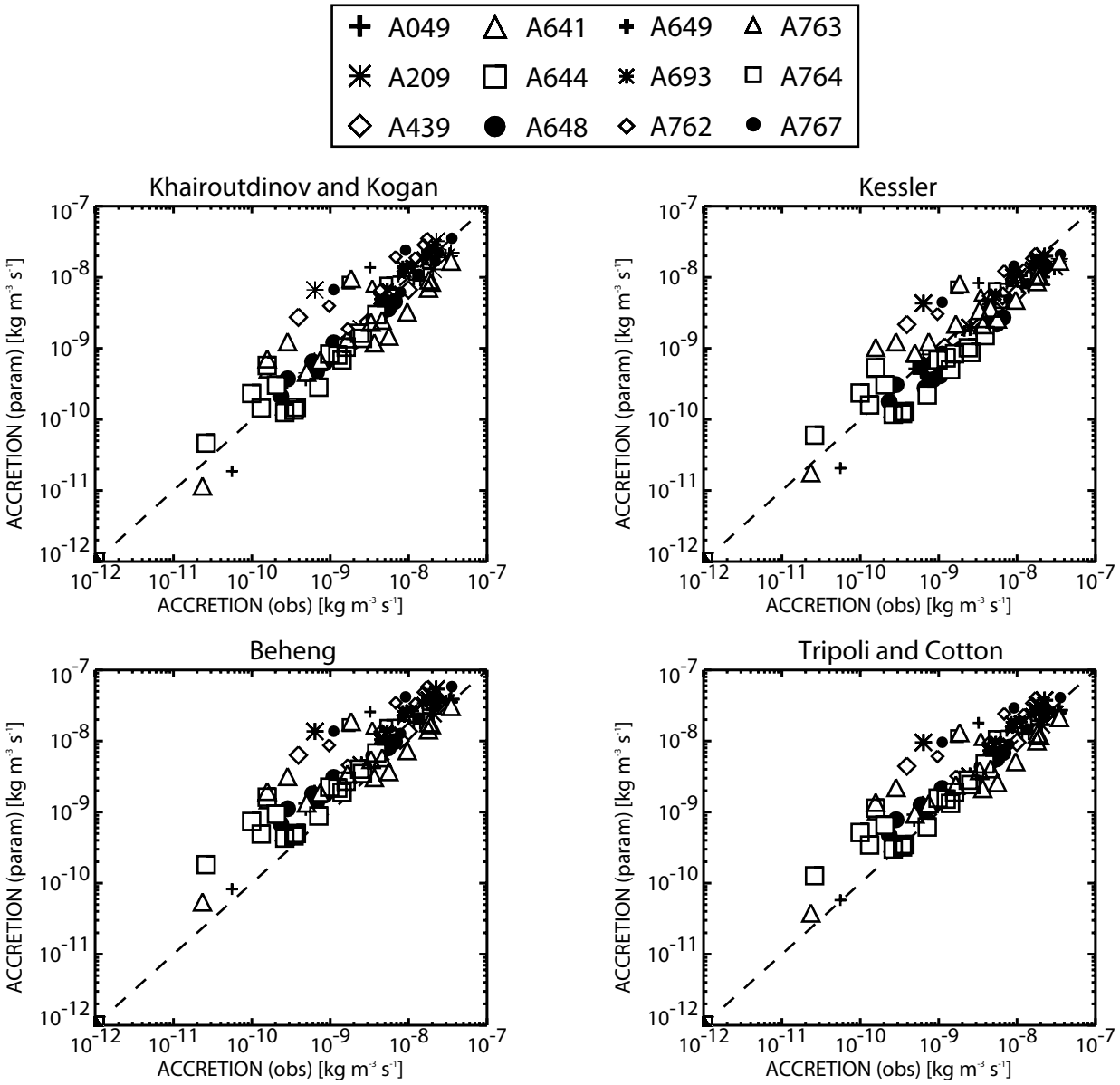
A049
A641
A649
A763
A209
A644
A693
A764
A439
A648
A762
A767
Khairoutdinov and Kogan
Kessler
Beheng
Tripoli and Cotton
ACCRETION (param) [kg m-3 s-1]
ACCRETION (obs) [kg m-3 s-1]
10-7
10-8
10-9
10-10
10-11
10-12

Figure 6:

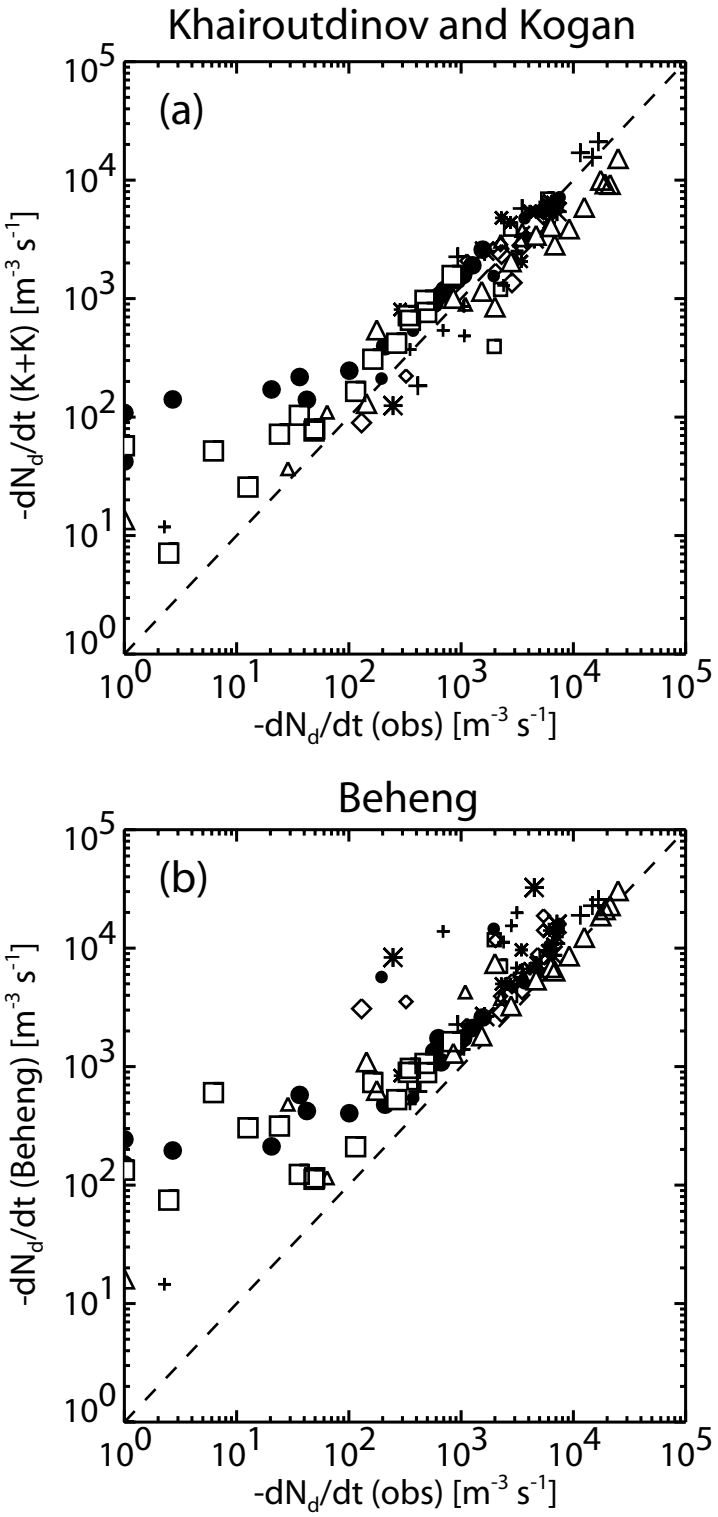
Khairoutdinov and Kogan
(a)
-dN$_d$/dt (K+K) [m^{-3} s^{-1}]
-dN$_d$/dt (obs) [m^{-3} s^{-1}]
Beheng
(b)
-dN$_d$/dt (Beheng) [m^{-3} s^{-1}]
-dN$_d$/dt (obs) [m^{-3} s^{-1}]

Figure 7:

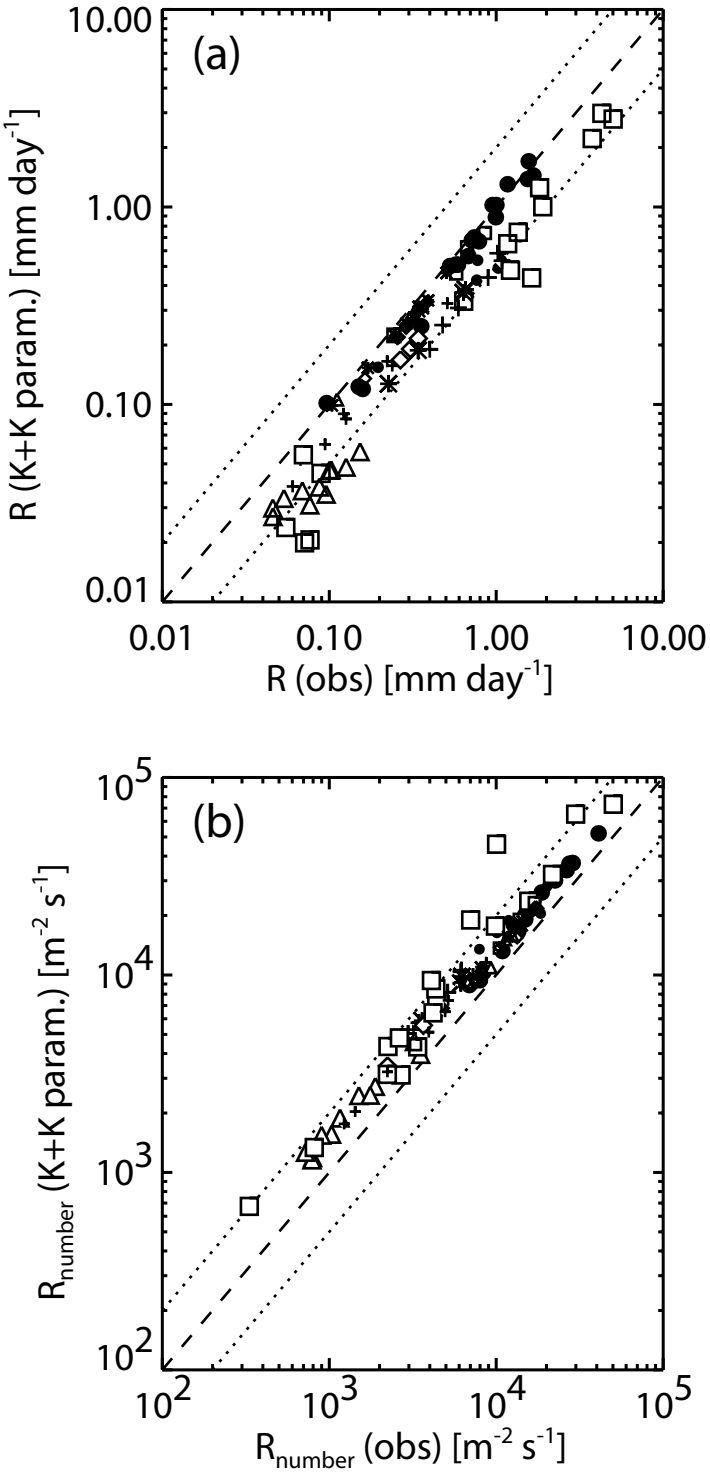
(a)
10.00
1.00
0.10
0.01
0.01
0.10
1.00
10.00
R (K+K param.) [mm day-1]
R (obs) [mm day-1]
(b)
10^5
10^4
10^3
10^2
10^2
10^3
10^4
10^5
R_number (K+K param.) [m-2 s-1]
R_number (obs) [m-2 s-1]

Figure 8:

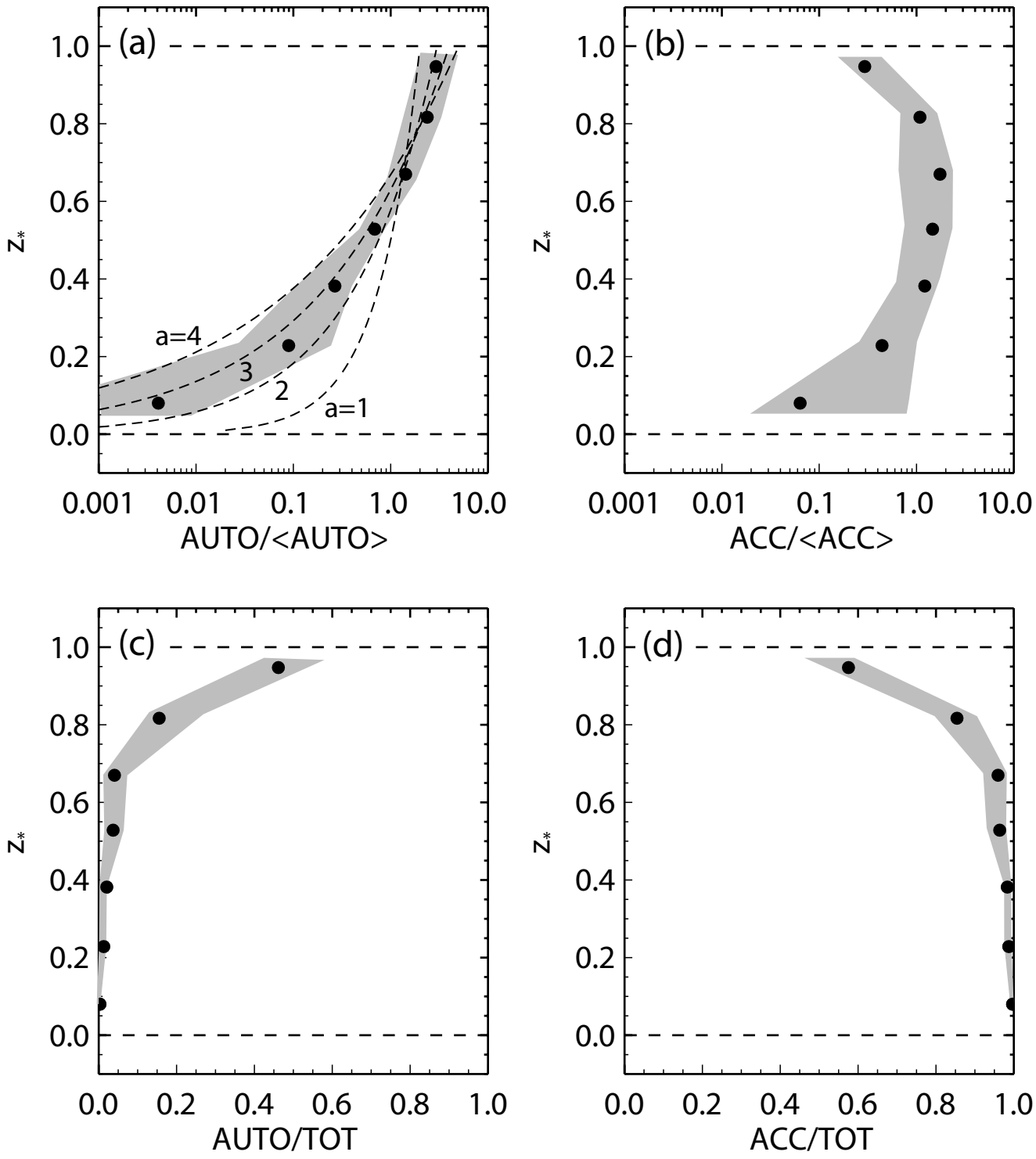
(a)
(b)
(c)
(d)
z*
AUTO/<AUTO>
ACC/<ACC>
AUTO/TOT
ACC/TOT
a=4
3
2
a=1
0.001
0.01
0.1
1.0
10.0
0.0
0.2
0.4
0.6
0.8

Figure 9:

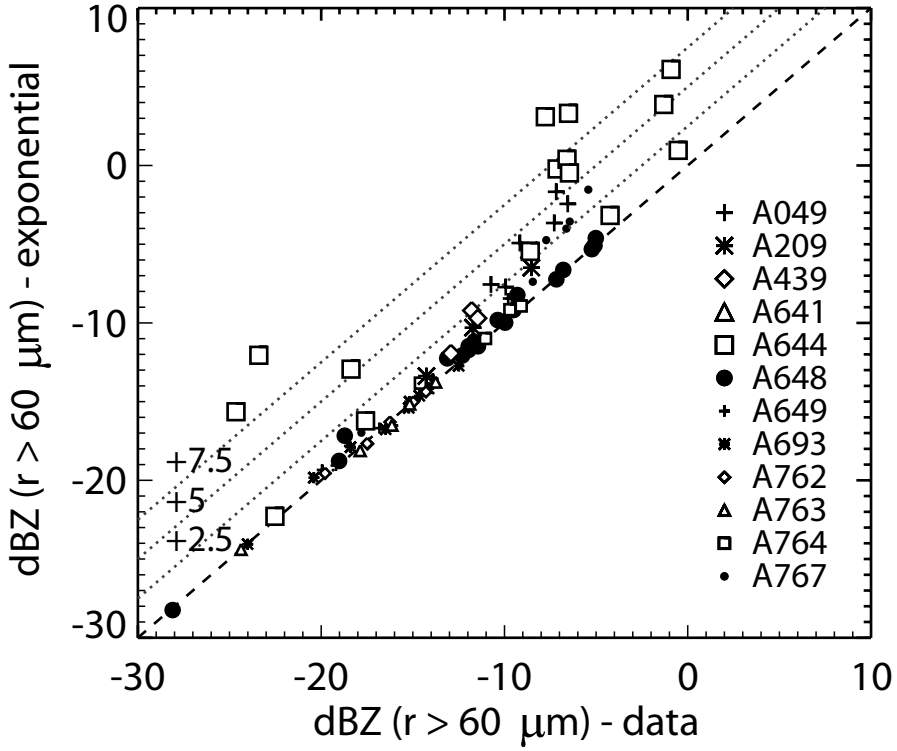
10
0
-10
-20
-30
-30
-20
-10
0
10
dBZ (r > 60 μm) - exponential
dBZ (r > 60 μm) - data
+7.5
+5
+2.5
A049
A209
A439
A641
A644
A648
A649
A693
A762
A763
A764
A767

Figure 10:

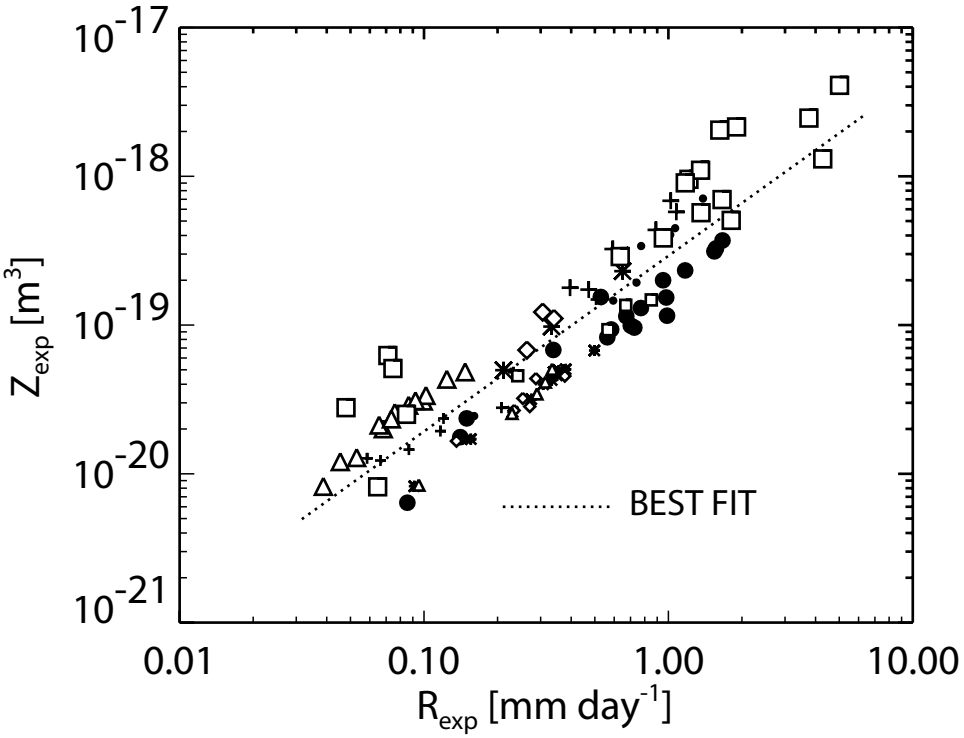
10-17
10-18
10-19
10-20
10-21
Zexp [m3]
BEST FIT
0.01
0.10
1.00
10.00
Rexp [mm day-1]

Figure 11: